Chem

CellPress

Article

A bulky 1,4,7-triazacyclononane and acetonitrile, a Goldilocks system for probing the role of Ni^{III} and Ni^{I} centers in cross-coupling catalysis

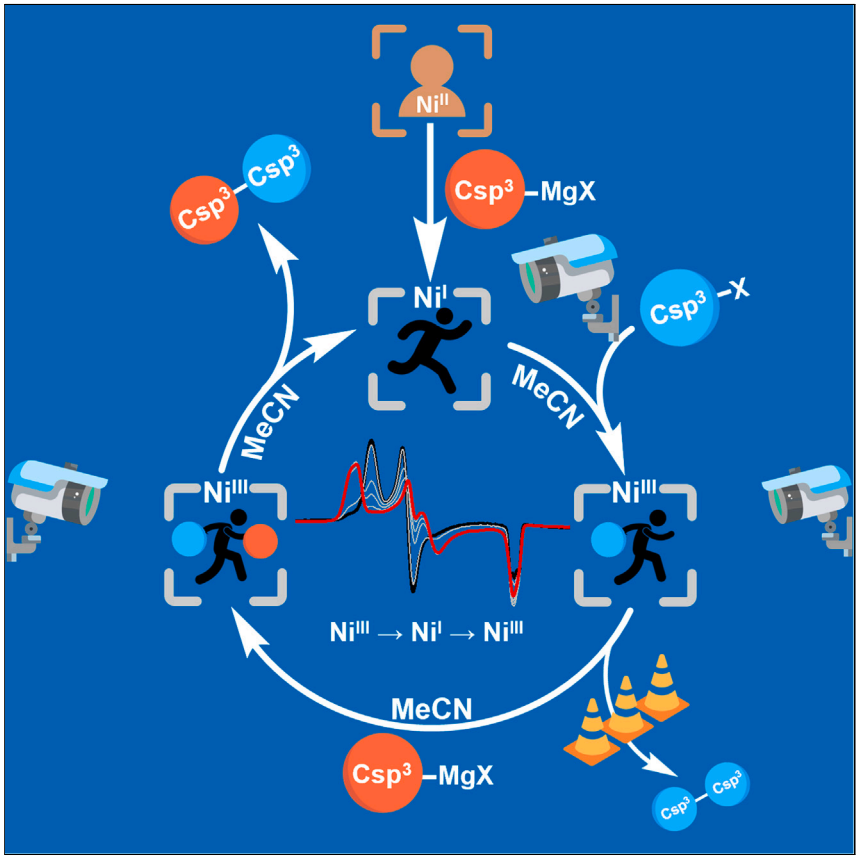

In nickel-catalyzed alkyl-alkyl cross-coupling reactions, paramagnetic Ni(I) and Ni(III) species are proposed to be the active intermediates. This study provides unambiguous evidence for the involvement of both Ni(III) and Ni(I) organometallic species in such cross-coupling reactions. In addition, the presence of acetonitrile or other alkyl nitriles improves the product yield in a multifaceted fashion, suggesting that the presence of a coordinating solvent and a weak π-acceptor, such as acetonitrile, could have a beneficial effect for a range of Ni-mediated organometallic transformations.

Leonel Griego, Ju Byeong Chae, Liviu M. Mirica

mirica@illinois.edu

Highlights

Detected or isolated organometallic Ni(I) and Ni(III) complexes were studied

Each step in the alkyl-alkyl Kumada cross-coupling was probed by EPR spectroscopy

The multifaceted beneficial role of acetonitrile during catalysis was investigated

Griego et al., Chem *10*, 867–881
March 14, 2024
https://doi.org/10.1016/j.chempr.2023.11.008

Chem

CellPress

Article

A bulky 1,4,7-triazacyclononane and acetonitrile, a Goldilocks system for probing the role of Ni^{III} and Ni^{I} centers in cross-coupling catalysis

Leonel Griego,[1,2] Ju Byeong Chae,[1,2] and Liviu M. Mirica[1,3,*]

SUMMARY

In nickel-catalyzed cross-coupling reactions involving alkyl substrates, catalysts supported by N-donor ligands are proposed to involve paramagnetic Ni(I) and Ni(III) species as key intermediates. Herein, we report the use of a bulky ligand, 1,4,7-triisopropyl-1,4,7-triazacyclononane (iPr_3TACN), that facilitated the detection or isolation of uncommon organometallic Ni(I) and Ni(III) complexes involved in well-defined oxidative addition, transmetalation, and reductive elimination steps. Moreover, (iPr_3TACN)Ni(II) complexes were shown to be efficient catalysts for alkyl-alkyl Kumada cross-coupling. The presence of acetonitrile and other alkyl nitriles led to an increased yield of cross-coupled products, and the multifaceted beneficial role of the nitrile additive during catalysis was thoroughly investigated. Overall, these studies provide unambiguous evidence for the involvement of both Ni(III) and Ni(I) organometallic species in Ni-catalyzed alkyl-alkyl cross-coupling reactions and suggest the presence of a coordinating solvent and a weak π-acceptor, such as acetonitrile, could have a beneficial effect for a range of Ni-mediated organometallic transformations.

INTRODUCTION

Cross-coupling reactions catalyzed by nickel complexes have become indispensable for the synthesis of new molecules with more complex structures and improved chemical and biological properties.[1–5] By comparison to the extensively developed Pd-catalyzed reactions, the Ni catalysts have the increased ability to employ alkyl electrophiles and nucleophiles and promote stereoselective transformations. For such alkyl-alkyl cross-coupling reactions, Ni complexes stabilized by bidentate and tridentate N-donor ligands have been shown to be the most efficient. For example, Fu, Hu, and Vicic groups have independently studied various organometallic Ni complexes supported by tridentate N-based ligand frameworks such as pyridinebisoxazolines, NNN pincer ligands, and terpyridine ligands, respectively (Figure 1).[5–12] In all these cases, a Ni^{III}-dialkyl species is proposed to be an active intermediate in the C–C coupling of alkyl electrophiles with various alkyl nucleophiles, yet no system has allowed the direct observation of any Ni^{III}-dialkyl species. Scorpionate tridentate ligands, such as $HCPy_3$ and $HBPz_3^-$ (Tp), have been used by Bour et al. to stabilize $LNi^{III}RR'$ species (where R/R′ = CF_3, biphenyl, Ar/CF_3, cycloneophyl, C_4F_8), yet no Ni^{III}-dialkyl species were isolated in those cases either.[13–15] Our group has previously isolated high-valent organometallic Ni species by using tetradentate pyridinophane ligands and ancillary CF_3 or cycloneophyl ligands to stabilize the Ni^{III} centers[16–20]; however, Ni^{III}-dialkyl complexes bearing a tridentate ligand have remained elusive to date.

THE BIGGER PICTURE

The last two decades have led to a dramatic development of nickel-catalyzed cross-coupling reactions involving alkyl substrates, including a wide range of stereoselective transformations. In these reactions, nickel complexes supported by N-donor ligands have been proposed to involve paramagnetic Ni(I) and Ni(III) species as the active intermediates during catalysis. Herein, we employed a bulky tridentate ligand to provide unambiguous evidence for the involvement of both Ni(III) and Ni(I) organometallic species in the three elementary steps of the proposed catalytic cycle: oxidative addition, transmetalation, and reductive elimination. In addition, the presence of acetonitrile and other alkyl nitriles led to an increased product yield, and this surprising effect was investigated in detail. Overall, these studies suggest the presence of a coordinating solvent and a weak π-acceptor, such as acetonitrile, could have a beneficial effect for a range of Ni-mediated organometallic transformations.

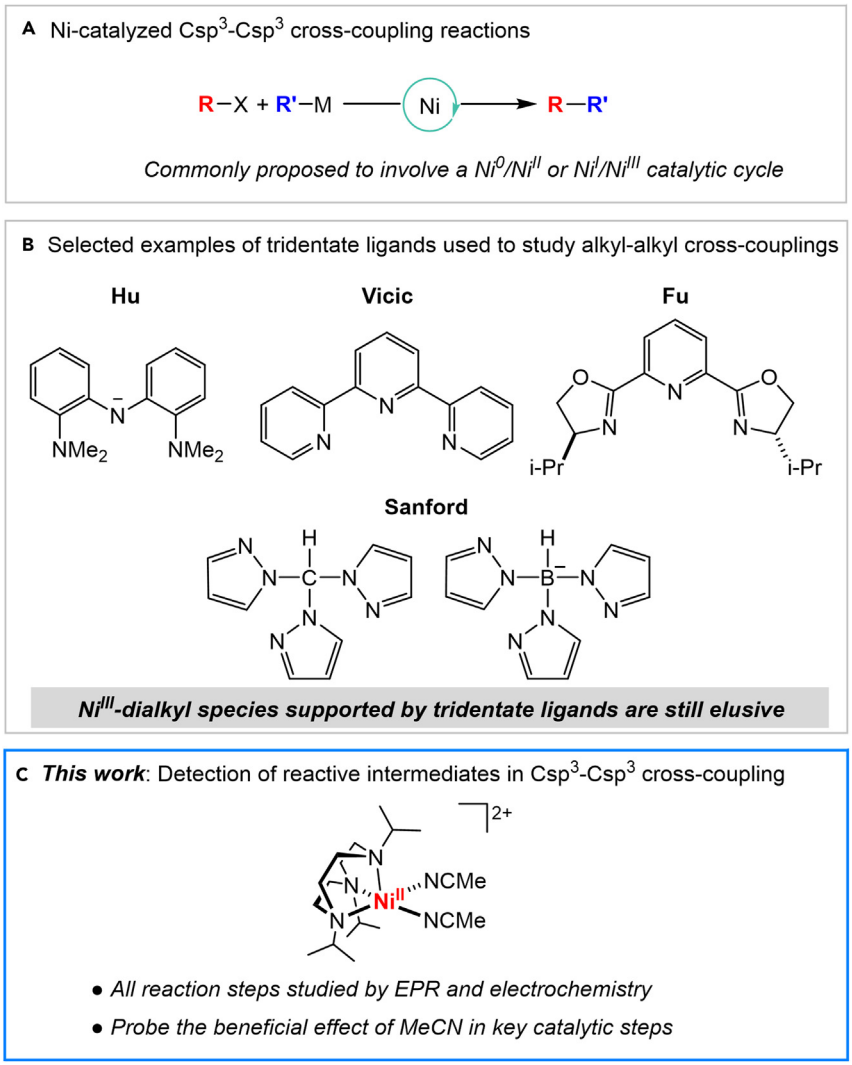

Figure 1. An overview of Ni-catalyzed Csp^3-Csp^3 cross-coupling reactions supported by tridentate ligands

(A) Depiction of a general Kumada cross-coupling reaction.

(B) Previously reported tridentate ligands used to study Csp^3-Csp^3 cross-couplings.

(C) Key findings reported herein.

Tridentate ligands based on the 1,4,7-triazacyclononane (TACN) azamacrocycle have been extensively used in bioinorganic chemistry to generate Fe and Cu complexes,[21–23] but only a few (TACN)Ni complexes have been reported to date.[24–26] We have previously reported the use of 1,4,7-trimethyl-TACN (Me_3TACN) to stabilize high-valent, organometallic Pd-dialkyl[27,28] and Ni-cycloneophyl[19] complexes. Attempts at making the Ni-dimethyl complex bearing this ligand framework remained elusive due to the tendency of its Ni-dihalide precursor to form a $[Ni^{II}(\mu\text{-}Cl)_3Ni^{II}]^+$ dinuclear species that inhibits transmetalation, which is essential for the synthesis of the dimethyl complex.[24] The steric effect of the N-substituents on the TACN system has been probed previously by using 1,4,7-triisopropyl-TACN (iPr_3TACN)[29] for the isolation and characterization of a mononuclear $NiCl_2$ complex. Recently, our group has reported the isolation of a Ni^I complex supported by iPr_3TACN and *tert*-butylisocyanide, $[(iPr_3TACN)Ni^I(CN^tBu)_2](PF_6)$; however, its organometallic reactivity has not been investigated.[30]

[1]Department of Chemistry, University of Illinois at Urbana-Champaign, 600 S. Mathews Avenue, Urbana, IL 61801, USA

[2]These authors contributed equally

[3]Lead contact

*Correspondence: mirica@illinois.edu

https://doi.org/10.1016/j.chempr.2023.11.008

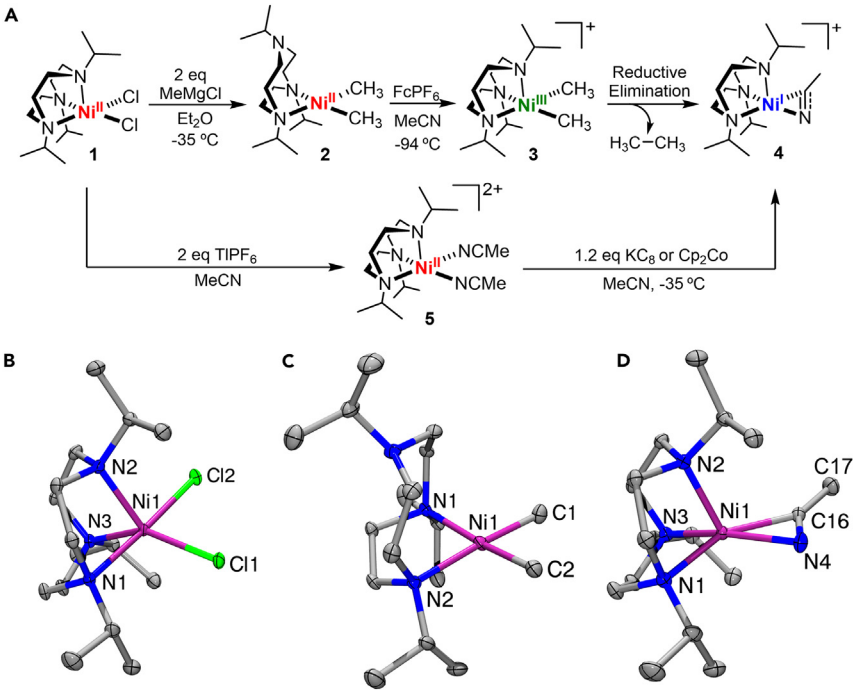

Figure 2. Synthesis and structural characterization of Ni complexes

(A) Synthesis of (iPr_3TACN)Ni complexes.

(B) Solid-state structure of **1** with 50% probability ellipsoids (hydrogen atoms omitted for clarity); selected bond lengths (Å): Ni1–N1 2.1879(9), Ni1–N2 2.0773(9), Ni1–N3 2.0965(9), Ni1–Cl1 2.2972(3), and Ni1–Cl2 2.3969(3).

(C) Solid-state structure of **2** with 50% probability ellipsoids (hydrogen atoms omitted for clarity); selected bond lengths (Å): Ni1–C1 1.933(4), Ni1–C2 1.937(4), Ni1–N1 2.089(4), and Ni1–N2 2.074(3).

(D) Solid-state structure of **4** with 50% probability ellipsoids (hydrogen atoms and counteranion omitted for clarity); selected bond lengths (Å) and angles (°): Ni1–N1 2.0764(14), Ni1–N2 2.0557(14), Ni1–N3 2.0534(14), Ni1–N4 1.9383(14), Ni1–C16 1.9153(17), N4–C16 1.206(2), and C17–C16–N4 142.35(13).

Herein, we report the synthesis, characterization, and reactivity studies of organometallic Ni^{I}, Ni^{II}, and Ni^{III} complexes supported by iPr_3TACN (Figure 2A). These complexes are involved in well-defined oxidative addition, transmetalation, and reductive elimination steps that are essential to the cross-coupling catalytic cycle. Mechanistic studies involving electron paramagnetic-resonance (EPR) spectroscopy, electrochemical methods, and radical clock substrates provide unambiguous evidence for a direct Csp^3-Csp^3 reductive elimination from Ni^{III} to Ni^{I}, oxidative addition of an alkyl halide via a radical mechanism from Ni^{I} and Ni^{III}, transmetalation at Ni^{III}, and the reduction of a Ni^{II} precatalyst to an active Ni^{I} species by the Grignard reagent. Moreover, (iPr_3TACN)Ni^{II} complexes were shown to be efficient catalysts for the alkyl-alkyl Kumada cross-coupling, and the presence of acetonitrile and other alkyl nitriles led to an increased yield of cross-coupled product. Although the beneficial role of nitriles (mostly aryl nitriles) in Ni catalysis has been reported previously, such a role was proposed to be due to the formation of Ni^{0}-nitrile adducts.[31–36] Herein, detailed spectroscopic, electrochemical, and mechanistic studies suggest that a weaker π-acceptor, such as acetonitrile, is able to slightly stabilize a Ni^{I} species while also preventing β-hydride elimination and promoting transmetalation and rapid reductive elimination from the Ni^{III} species. Overall, these studies provide unambiguous evidence for the involvement of both Ni^{III} and Ni^{I} organometallic species in Ni-catalyzed alkyl-alkyl cross-coupling reactions and also suggest that the

presence of a coordinating solvent and a weak π-acceptor, such as acetonitrile, could have a beneficial effect for a range of Ni-mediated organometallic transformations involving Ni^{I} intermediates.

RESULTS AND DISCUSSION

Synthesis and characterization of (iPr_3TACN)Ni complexes

The (iPr_3TACN)$Ni^{II}Cl_2$ complex (**1**) was synthesized upon the metalation of iPr_3TACN with $NiCl_2$(DME) in 91% yield (Figure 2A).[30] Yellow X-ray quality crystals were obtained, and the solid-state structure revealed a five-coordinate Ni^{II} center (Figure 2B). A closer look reveals two Ni–N bonds with similar bond lengths of 2.077 and 2.096 Å, whereas the third N atom is positioned at 2.188 Å from the Ni center. The geometry index of τ_5 = 0.48 indicates that the Ni center adopts a geometry between square pyramidal and trigonal bipyramidal, giving rise to inequivalent Ni–Cl bond lengths that differ by ~0.1 Å. The disparity between these two Ni–Cl bond lengths is intriguing, since it is indicative of a potentially labile halide. Moreover, the cyclic voltammogram (CV) reveals an oxidation event at $E_{1/2}$ = +0.68 V vs. Fc^{+}/Fc, presumably corresponding to a Ni^{II}/Ni^{III} redox couple (Figure S17).

The mononuclear nature of complex **1** allowed for its reaction with 2 equiv CH_3MgCl to afford (iPr_3TACN)$Ni^{II}(CH_3)_2$ (**2**, Figure 2A). Extraction with pentane and concentration of the solution at −35°C afforded X-ray quality yellow crystals of **2** in 61% yield. The solid-state structure reveals a square planar Ni^{II} center, with the iPr_3TACN ligand binding in a bidentate fashion with Ni–N bond lengths of 2.089 and 2.074 Å, and two ancillary methyl groups with Ni–C bond lengths of 1.933 and 1.937 Å (Figure 2C). As expected, the CV of the dimethyl complex **2** reveals more accessible oxidation events than those observed for the dihalide complex **1** (Figure S18). Two irreversible oxidation events, presumably corresponding to the Ni^{II}/Ni^{III} and Ni^{III}/Ni^{IV} redox couples, are observed at E_{pa} = −0.62 V and +0.01 V vs. Fc^{+}/Fc, respectively.

We then tested the oxidative reactivity of **2** by monitoring the formation of ethane upon oxidation with various one-electron and two-electron oxidants (Figures 3A and S25–S30). Reaction of **2** with 1 equiv $FcPF_6$ generated ethane cleanly in 88% yield after 20 min at −20°C in CD_3CN. In addition, when **2** was reacted with 2 equiv of the milder oxidant Fc*PF_6 ($E_{1/2}$ = −0.59 V vs. Fc^{+}/Fc), a similar yield of 89% ethane was obtained (Figure 3A), suggesting that the generation of a Ni^{IV} intermediate is not needed for efficient C–C bond formation, whereas a second equivalent of this mild oxidant is not needed to oxidize the resulting Ni^{I} product in order to alleviate unwanted side reactions, as employed previously.[13] The same reaction performed in tetrahydrofuran-d_8 (THF-d_8) afforded ethane in 79% yield and methane in 19%, suggesting a cleaner reductive elimination of ethane in the presence of MeCN. Excitingly, the oxidation of **2** with the O-based oxidants H_2O_2, urea·H_2O_2, and even O_2 led to a rapid formation of ethane in ~90% yield (Figures 3A and S30). Overall, the observed fast and selective oxidatively induced C–C bond formation in the presence of O-based oxidants suggests that such oxidation processes could be employed in catalytic transformations.

We then investigated the mechanism of C–C bond formation product using complexes **2** and its CD_3 analog **2-CD_3** to perform crossover experiments (Figures 3B and S31). Interestingly, oxidation of a 1:1 mixture of **2** and **2-CD_3** with various one- and two-electron oxidants generated only ethane and d_6-ethane, with no CH_3-CD_3 being observed. This is in contrast to previous results obtained for a (^{Me}N4)$NiMe_2$ complex supported by a tetradentate pyridinophane ligand, in which

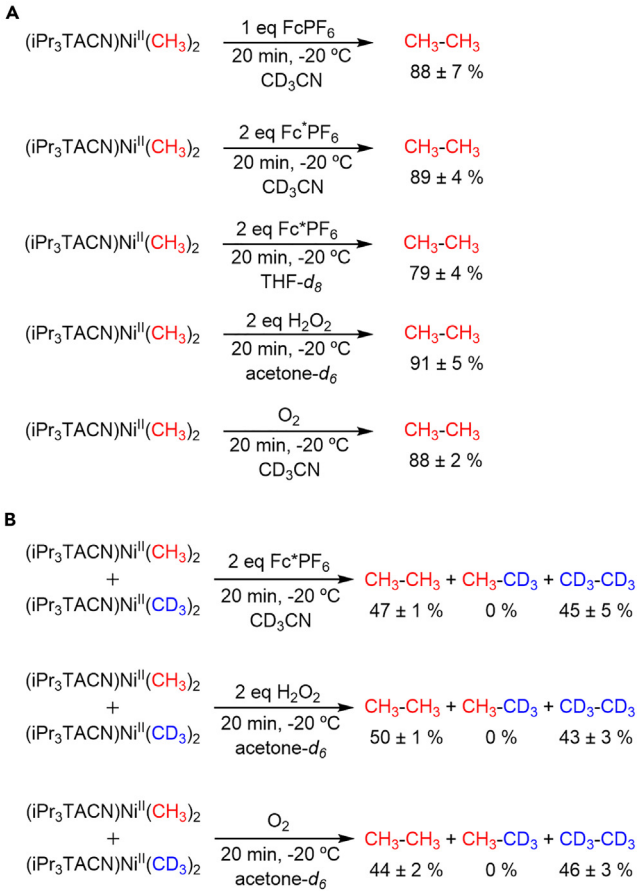

Figure 3. C–C bond formation reactivity studies

(A) Yields of ethane formed upon the oxidation of **2** with various oxidants, obtained by ^{1}H NMR with trimethoxybenzene as an internal standard.

(B) Yields of ethane isotopologs formed upon the oxidation of **2** with various oxidants, obtained by ^{1}H and ^{2}H NMR with trimethoxybenzene or toluene-d_8 as an internal standard, respectively.

the CH_3-CD_3 crossover product was formed via a proposed methyl group transfer mechanism involving a (^{Me}N4)Ni^{IV}Me$_3$ intermediate.[18] In a later study, the use of a pseudo-tridentate pyridinophane ligand ^{MeTs}N4 did not generate the CH_3-CD_3 crossover product upon oxidation of the corresponding (^{MeTs}N4)NiMe$_2$ complex, and a transient 5-coordinate Ni^{III}Me$_2$ intermediate was proposed to undergo rapid reductive elimination of ethane and formation of a Ni^{I} complex.[20] For these pyridinophane systems, the generated Ni^{I} species are unstable and undergo rapid disproportionation to Ni^{0}, free ligand, and a Ni^{II}-solvento complex, precluding any appreciable alkyl-alkyl cross-coupling catalysis.[16,18–20] In the case of **2**, we propose the formation of a 5-coordinate Ni^{III}Me$_2$ species that undergoes rapid C–C bond formation to eliminate ethane. Importantly, in the current system, no Ni^{0} formation or further decomposition was observed upon ethane formation in MeCN.

Given the rapid oxidatively induced reactivity of **2**, we then sought to detect any transient high-valent Ni intermediates. Gratifyingly, when **2** was reacted with 1 equiv $FcPF_6$ at −94°C in THF:2-MeTHF, a rhombic EPR spectrum was observed and assigned to the [(iPr$_3$TACN)Ni^{III}Me$_2$]$^{+}$ (**3**) species. The EPR spectrum is representative of a square pyramidal d^7 Ni^{III} center and was simulated using g values of 2.379, 2.271, and 2.009 (Figure 4A, black), along with superhyperfine coupling in the g_z

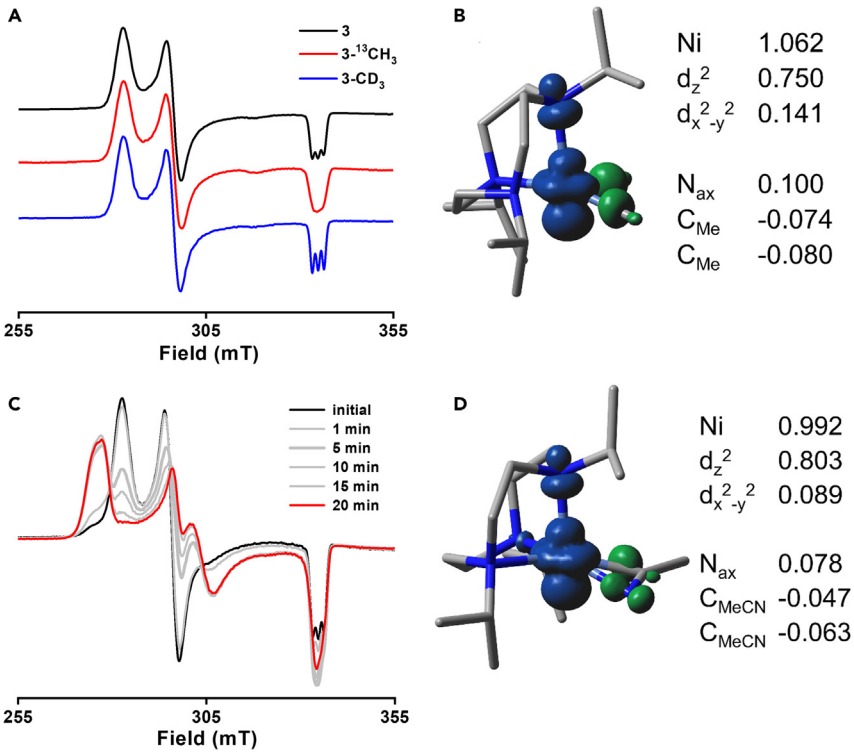

Figure 4. EPR characterization of Ni^{III} and Ni^{I} species

(A) Stacked EPR spectra (1:5 THF:2-MeTHF glass, 77 K) of Ni^{III} species formed upon the oxidation of the Ni^{II} precursors with $FcPF_6$ at −94°C. Simulation parameters for **3**: g_x = 2.378, g_y = 2.269, g_z = 2.010 (A_N = 16.0 G).

(B) DFT-calculated Mulliken spin density for **3**, shown as a 0.05 isodensity contour plot.

(C) EPR spectra (1:5 MeCN:PrCN glass, 77 K) at different time points at −20°C, monitoring the conversion of **3** to **4** upon reductive elimination of ethane.

(D) DFT-calculated Mulliken spin density for **4**, shown as a 0.05 isodensity contour plot.

direction corresponding to one N atom (I = 1, A_N = 16 G), likely due to the axial N donor from the iPr_3TACN ligand.[16,18–20] To provide further evidence that the methyl groups are still bound to the Ni center, we synthesized the ^{13}C-labeled complex (iPr_3TACN)$Ni^{II}(^{13}CH_3)_2$ (**2-^{13}CH$_3$**), along with **2** and **2-CD$_3$** (Figure 4A). Oxidation of these three isotopologs generated Ni^{III} species exhibiting EPR spectra that are significantly different, especially in the g_z region, as the superhyperfine coupling pattern either gets broadened or narrowed for **3-^{13}CH$_3$** and **3-CD$_3$**, respectively (Figure 4A). For **3-^{13}CH$_3$**, an appropriate simulation of the EPR spectrum required additional superhyperfine coupling to ^{13}C (A_{13C} = 10 G) in the g_z direction (Figures S32–S34). A similar trend has previously been observed by Manesis et al. for a protein-based M121A AzNi^{III}-methyl system, for which superhyperfine coupling broadening was observed for the $^{13}CH_3$ isotopolog, whereas a narrowing effect of the coupling pattern was observed for the CD_3 isotopolog, due to the significantly smaller gyromagnetic ratio of ^{2}H (D) vs. ^{1}H.[37,38] In our case, density functional theory (DFT) calculations further support the electronic properties and the simulation of the EPR spectrum of **3**, with the calculated Mulliken spin density revealing that the unpaired electron resides mainly on the Ni center, with an appreciable contribution from the axial N atom (Figure 4B).

Multiple attempts to isolate complex **3** were unsuccessful due to its quick thermal decomposition. In a fortuitous attempt to crystallize the Ni complex with MeCN as

the solvent, we obtained an X-ray quality crystal corresponding to the [(iPr_3TACN)Ni^{I}(η^2-MeCN)]$^+$ complex (**4**, Figure 2A). This rare five-coordinate Ni^{I} complex is supported by three N-donor atoms of iPr_3TACN and one MeCN molecule that is bound in a side-on η^2 coordination mode.[39] The iPr_3TACN-Ni interactions in **4** were elongated compared with those in **3**, with Ni–N bond distances 2.076, 2.056, and 2.053 Å (Figures 2A–2D), consistent with a more electron-rich metal center.[39] Importantly, to the best of our knowledge, no Ni^{I}(η^2-MeCN) complex has been reported to date. Although several Ni^0 complexes with η^2-bound aryl nitriles have been reported,[31,33,40–43] the very few isolated Ni^0(η^2-alkylnitrile) complexes are either dinuclear[44] or multinuclear metal clusters,[45] or the alkyl nitrile is rendered more electron deficient via interaction with a Lewis acid.[46,47] For example, in the Ni^0(η^2-acetonitrile)(BEt_3) complex reported by Ateşin et al.,[46] the η^2-MeCN ligand displays a bent structure with a bond angle of 137.99° and an elongated nitrile C≡N bond of 1.234 Å, whereas for **4**, a nitrile C≡N bond of 1.206 Å and a N≡C–C bond angle of 142.35° is observed, consistent with a less electron-rich Ni^{I} metal center that exhibits a lesser degree of π back-bonding.

Interestingly, monitoring by EPR of the oxidation of complex **2** with $FcPF_6$ in the presence of a nitrile solvent allowed for the direct observation of the reductive elimination of ethane from **3** to generate **4**. The short-lived complex **3** was observed by lowering the temperature of the oxidation of **2** with $FcPF_6$ to −94°C in 1:3 MeCN:PrCN. Importantly, warming up the reaction mixture to −20°C and freeze quenching at various time points allowed for the complete formation of **4** after 20 min (Figure 4C), and this direct two-electron transformation from **3** to **4** correlated with the formation of ethane, as quantified by ^{1}H NMR (Figure S35). By contrast, the oxidation reaction in the absence of nitrile solvents (THF:2-MeTHF) at −94°C and subsequent warmups at −20°C resulted in the decomposition of **3**, without formation of **4** (Figure S36); instead, the formation of Ni^0 as a black powder was observed. Importantly, this result highlights the importance of a nitrile solvent to form a stabilized Ni^{I} complex. In several reports, benzonitrile and nitrile additives[31–33,48] or nitrile-containing ligands[35,49,50] were shown to stabilize Ni^0 species during catalysis and favor reductive elimination and disfavor β-hydride elimination,[35] whereas acetonitrile was proposed to destabilize a Ni^0 intermediate in one case and lead to increased catalytic activity and a broader substrate scope.[34]

We then sought to confirm the formation of the Ni^{I}(η^2-MeCN) complex **4** by direct synthesis via the reduction of the isolable Ni^{II} precursor [(iPr_3TACN)Ni^{II}($MeCN)_2$]$_2^+$ (**5**), which can be obtained by halide abstraction from **1** with 2 equiv $TlPF_6$.[30] The CV of **5** shows a Ni^{II}/Ni^{I} reduction couple at $E_{1/2}$ = −1.30 V vs. Fc^+/Fc (Figure S19), and reduction of **5** with KC_8 or $CoCp_2$ generates an identical EPR signal to that of **4**, observed upon the oxidatively induced ethane elimination from **2** (Figure S37). The EPR spectrum was simulated with g values of $g_x \approx 2.44$, $g_y \approx 2.24$, and $g_z \approx 2.01$ ($A_N \approx 12$ G, Figures S38 and S39), comparable with the DFT-calculated g values of 2.428, 2.201, and 2.035 for **4** (Table S1), whereas the calculated Mulliken spin density for **4** suggests the unpaired electron resides in a Ni-based d_z^2 orbital (Figure 4D; Tables S10 and S11). Notably, the rhombic EPR spectrum of **4** is different from the axial EPR spectra observed recently for a TACN-supported Ni^{I} species that does contain an acetonitrile ligand.[51,52]

Kumada Csp^3-Csp^3 cross-coupling reactions

Nickel catalysts are commonly used for Csp^3-Csp^3 cross-coupling reactions, and Ni^{I} and Ni^{III} species are usually proposed as the key intermediates during the catalytic

Table 1. Stoichiometric cross-coupling reactions

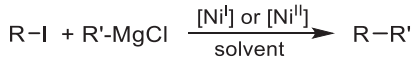

R-X	R′-MgCl	[Ni][a]	Solvent	R-R′ yield[b]
Me-I	*n*-octyl-MgCl	**4** (Ni^{I})	1:9 MeCN:THF	50 %
Me-I	*n*-octyl-MgCl	**5** (Ni^{II})	1:9 MeCN:THF	47 %
Me-I	*n*-octyl-MgCl	**5** (Ni^{II})	THF	15 %
n-Heptyl-I	*n*-octyl-MgCl	**4** (Ni^{I})	1:9 MeCN:THF	39 %
n-Heptyl-I	*n*-octyl-MgCl	**5** (Ni^{II})	1:9 MeCN:THF	42 %
n-Heptyl-I	*n*-octyl-MgCl	**5** (Ni^{II})	THF	14 %

[a][Ni] = [(iPr_3TACN)Ni^{I}(η^2-MeCN)]$^+$ (**4**) or [(iPr_3TACN)Ni^{II}(MeCN)$_2$]$^{2+}$ (**5**). **4** was prepared *in situ* by reacting **5** with 1 equiv of KC_8 at −35°C, followed by removal of insoluble byproducts through filtration.
[b]The Grignard (1.5 equiv) and alkyl electrophile were added simultaneously at −35°C, and the reaction was allowed to stir to room temperature (RT) for 1 h. Yields were determined using GC-mass spectrometry (MS) with dodecane as the internal standard and represent average values of at least three independent measurements, and the homocoupled products tetradecane and hexadecane were formed in less than 5% yield.

cycle.[2,3,5] Although either organometallic Ni^{I} or Ni^{III} species have been observed as intermediates in catalytic processes, to the best of our knowledge, no system that can allow the detection of both organometallic Ni^{I} or Ni^{III} species in the same catalytic process has been reported to date. In this context, we first probed the stoichiometric cross-coupling reactivity of the Ni^{I} complex **4**. From the EPR studies, we learned that the presence of acetonitrile was essential for the stabilization of **4**, and thus, a 1:9 MeCN:THF solvent mixture was employed in the reaction of **4** with either MeI or *n*-heptyl-iodide (I) and 1.5 equiv of *n*-octylMgCl to generate nonane or pentadecane in 50% and 39% yields, respectively (Table 1, entries 1 and 4). In addition, the reaction of the Ni^{II}-solvento complex **5** with either MeI or *n*-heptyl-I and 1.5 equiv of *n*-octylMgCl also generated nonane or pentadecane in 47% and 42% yields, respectively (Table 1, entries 2 and 5), suggesting that reduction to a Ni^{I} species in the presence of a Grignard can occur *in situ* (see below). Surprisingly, performing the reactions in neat THF led to a significant decrease in the yields of nonane and pentadecane to 15% and 14%, respectively (Table 1, entries 3 and 6), suggestive of a beneficial role of MeCN in promoting efficient C–C bond formation.

Intrigued by the beneficial effect of acetonitrile during the stoichiometric cross-coupling studies, we then probed the catalytic Kumada Csp^3-Csp^3 cross-coupling using the Ni^{II}-solvento complex **5** as the precatalyst and optimized the reaction conditions (Table 2). All product yields were corrected with calibration curves and experimentally determined response factors, using dodecane as an internal standard (see section GC method conditions for cross-coupling reactions of the supplemental information; Figures S43–S48). The calibration of the product yields has proved to be essential as the alkane products seem to consistently exhibit reduced response factors, and thus, without calibration, the product yields are significantly overestimated.[53] Interestingly, **5** showed a strong dependence on the amount of MeCN present in the solvent mixture. Compared with the neat THF conditions, the addition of MeCN up to a 1:1 MeCN:THF ratio (i.e., 200 equiv MeCN) produced up to 85% yield of pentadecane, whereas higher amounts of MeCN lowered the product yield (Table 2, entries 4–8; Figure 5A). Notably, the byproduct 1-decanone, generated from the reaction between MeCN and *n*-octylMgCl and subsequent aqueous workup, was not observed during the catalytic runs.[54] The use of (iPr_3-TACN)$Ni^{II}Cl_2$ or (iPr_3TACN)$Ni^{II}Br_2$ as catalysts led to slightly lower product yields (Table 2, entries 9 and 10), which plateaued at a lower MeCN:THF ratio (Figure 5A). Importantly, use of the *in situ*-generated Ni^{I} species **4** as the catalyst generated a similar

Table 2. Reaction optimization for the Csp^3-Csp^3 Kumada cross-coupling catalyzed by $[(iPr_3TACN)Ni^{II}(MeCN)_2]^{2+}$ (5)

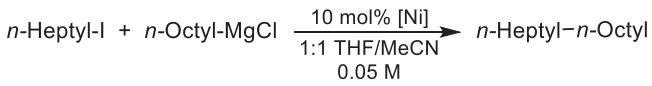

Entry	Variation from the standard conditions[a]	Yield (%)[b]
1	none	**85 ± 4**
2	without Ni catalyst	0
3	THF (no MeCN)	28 ± 2
4	1 equiv MeCN	34 ± 3
5	10 equiv MeCN	46 ± 3
6	7:1 THF/MeCN (50 equiv MeCN)	62 ± 4
7	3:1 THF/MeCN (100 equiv MeCN)	82 ± 3
8	1:3 THF/MeCN (300 equiv MeCN)	52 ± 4
9	$(iPr_3TACN)Ni^{II}Cl_2$ instead of **5**[c]	66 ± 3
10	$(iPr_3TACN)Ni^{II}Br_2$ instead of **5**[c]	65 ± 2
11	**4** instead of **5**[d]	83 ± 3

[a]Standard conditions: *n*-heptyl iodide (0.1 mmol, 1.0 equiv), **5** (10 mol %), MeCN (1.0 mL, 200 equiv), *n*-octylMgCl (0.15 mmol, 1.5 equiv), 0.5 mL THF, 2 h, RT.
[b]Yields were obtained by GC-MS and were corrected using calibration curves, using dodecane as an internal standard, and represent average values of at least three independent measurements.
[c]Optimal yields were obtained in 7:1 THF/MeCN (50 equiv MeCN).
[d]**4** was prepared *in situ* by reacting **5** with 1 equiv of KC_8 at −35°C, followed by removal of insoluble by-products through filtration.

product yield vs. when complex **5** was used (Table 2, entry 11). Finally, when an alkyl bromide was used as the electrophile, a lower product yield was observed (Table S2, entries 12 and 13), whereas the Ni complexes formed *in situ* with a series of other Ni salts generated the cross-coupled product in acceptable yields (Table S4).To test the generality of the beneficial effect of MeCN in Ni-mediated Csp^3-Csp^3 Kumada cross-coupling, we screened a range of N-based ligands with different denticities and steric bulk under identical reaction conditions (Table S5). In our optimized conditions, we found that tridentate ligands having medium steric bulk such as iPr_3TACN (L1), Me_3TACN (L2), terpyridine (L15), and ^{i}Pr-Box (L16) showed an increase in the desired product in the presence of MeCN, whereas structurally crowded tridentate ligands

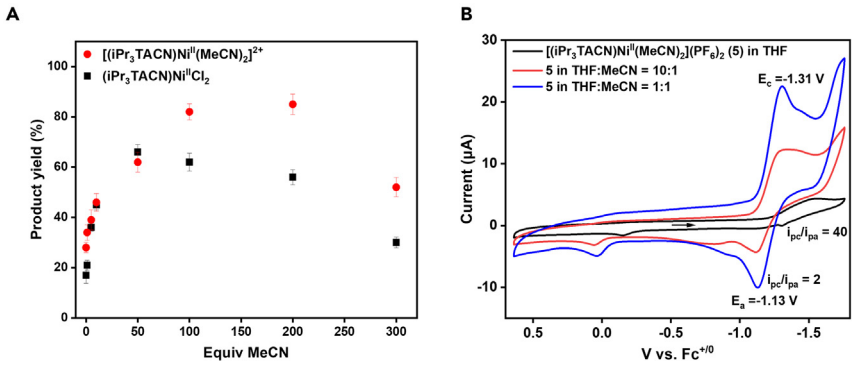

Figure 5. Effect of MeCN on catalytic and electrochemical properties of Ni complexes
(A) Plots of coupled product yields vs. amount of MeCN present in solution for the catalysts $(iPr_3TACN)Ni^{II}Cl_2$ (**1**, black squares) and **5** (red circles). Error bars are shown as 90% confidence intervals based on the average of 3 trials.
(B) Cyclic voltammograms (100 mV/s scan rate) of 1 mM **5** in 0.1 M *n*-Bu_4NPF_6 in THF (black), 10:1 THF:MeCN (red), and 1:1 THF:MeCN (blue). Note: complex **5** is only slightly soluble in THF.

(L3, L7, L8, and L14), bidentate, and tetradentate ligands[16,20,55–58] showed similar or lower cross-coupled product yield in the presence of MeCN (Table S5). Overall, these reactivity studies suggest a range of Ni cross-coupling catalysts supported by tridentate ligands could benefit from the presence of MeCN to generate improved product yields.

Probing the role of nitrile additives

To get a better understanding of the MeCN effect, we performed CV experiments in different solvent mixtures and different scan rates (Figures 5B, S21, and S22). The CV of **5** in *n*-Bu_4NPF_6/THF shows a quasi-reversible reduction wave at $E_{1/2} = -1.42$ V vs. Fc^+/Fc (ΔE_p = 220 mV), and a peak current ratio (i_{pc}/i_{pa}) of 40 suggests that the reduced species is not stable enough on the CV time scale to be re-oxidized. Interestingly, the i_{pc}/i_{pa} ratio significantly decreases with increasing amounts of MeCN, up to a ratio of ~2 in 1:1 THF/MeCN (Figure 5B), suggesting that the reduced Ni^I species is stabilized by MeCN. Moreover, the reductive peak is shifted to less-negative potentials from −1.54 to −1.33 V, supporting that Ni^I is more accessible in the presence of MeCN, whereas variable scan rate CV studies of **5** suggest a homogeneous process in solution that follows a non-Nernstian electrochemical-chemical (EC) mechanism (Figures S21 and S22). The same trend was observed for the dichloride complex **2**, although a higher amount of MeCN was needed to get a lower i_{pc}/i_{pa} ratio (Figures S20, S23, and S24), as expected, given the presence of chloride anions that compete with MeCN in binding to the Ni center.

In addition to stabilizing a reactive Ni^I species, the improved product yield in the presence of MeCN might be due also to the prevention of side reactions such as β-hydride elimination. Indeed, the amounts of β-hydride eliminated products heptene and octene were significantly reduced as the amount of MeCN increased (Figure S49). This might be due to the binding of MeCN into an open coordination site of the Ni center, thus preventing an agostic interaction with a C–H bond of the alkyl group that is necessary for β-hydride elimination. Since MeCN is a weak ligand, solvent amounts seem to be necessary to increase the effective concentration of the nitrile-bound Ni species. Based on these results, the presence of MeCN may lead to an increased cross-coupled product yield not only due to the slight stabilization of the Ni^I species in the presence of MeCN[31–33,48] but also due to the MeCN prevention of β-hydride elimination and promotion of a faster reductive elimination from the Ni^{III} species (Figures 3A, S26, and S27).

Finally, we postulated that other π-acid additives capable of stabilizing the Ni^I species could potentially promote product formation. First, the addition of alkyl nitriles such as butyronitrile (PrCN) and pivalonitrile (tBuCN) also improved the product yields vs. the reaction conducted in THF (Table S3, entries 3 and 4). Surprisingly, different benzonitriles reduced the product yield, and the electrophile was not fully consumed during the reaction, implying that the stronger π-accepting nature of benzonitrile may stabilize too much the Ni^I species and thus significantly slow down the oxidative addition step (Table S3, entries 5–7). Other π-acids such as styrenes and dimethyl fumarate completely suppressed the reaction when present in excess amounts (Table S3, entries 8–10). Inspired by a recent report,[59] we also tested whether dinitriles could improve the product yields. Malononitrile, a geminal dinitrile, completely quenched the reaction, suggesting that both nitrile groups might bind to the Ni^I center to generate a catalytically inactive species, whereas succinonitrile slightly improved the product formation (Table S3, entries 11 and 12).

Mechanistic studies

Considering that both stoichiometric and catalytic reactivity studies reveal the Ni^{II} species **5** and the Ni^I species **4** yield similar amounts of cross-coupled product—

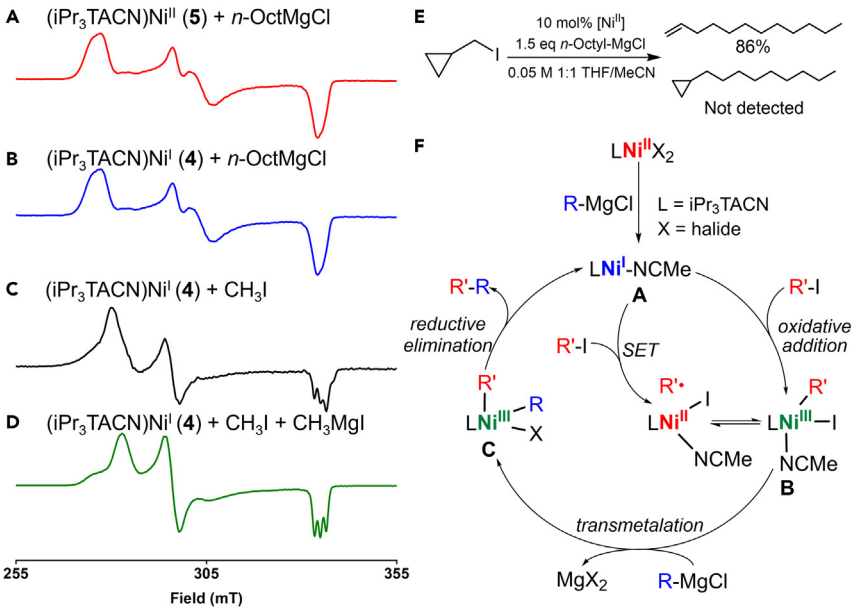

Figure 6. Mechanistic studies of the Kumada Csp^3-Csp^3 cross-coupling reaction

(A) EPR spectrum of $[(iPr_3TACN)Ni^{II}(MeCN)_2]^{2+}$ (**5**) + 1 equiv *n*-octylMgCl in 1:3 MeCN:PrCN at 77 K, generating **4**.

(B) EPR spectrum of $[(iPr_3TACN)Ni^{I}(\eta^2\text{-MeCN})]^{+}$ (**4**) + 1 equiv *n*-octylMgCl in 1:3 MeCN:PrCN at 77 K.

(C) EPR spectrum of **4** + 10 equiv CH_3I in 1:3 MeCN:PrCN at 77 K.

(D) EPR spectrum of **4** + 10 equiv CH_3I + 1 equiv CH_3MgI in 1:3 MeCN:PrCN at 77 K.

(E) Radical clock experiment (yields were measured by gas chromatography (GC)).

(F) Proposed mechanism for the Csp^3-Csp^3 Kumada cross-coupling for the $(iPr_3TACN)Ni^{II}$ system.

with a slightly faster product formation observed for **4** (Figure S50)—and a range of Ni^{II} precatalysts are competent in the Kumada cross-coupling reaction, we proposed that the catalytically active Ni^{I} species could be generated *in situ* via the reduction of the Ni^{II} precursor by the Grignard reagent. Indeed, the addition of either 1 equiv *n*-OctMgCl or 1 equiv CH_3MgCl to **5** led to the formation of the Ni^{I} complex **4**, as observed by EPR spectroscopy, suggesting that the Grignard reagent can reduce Ni^{II} to Ni^{I} *in situ* (Figure 6A). Moreover, both the Ni^{II}-solvento complex **5** and the Ni^{II}-dihalide complex **1** can be reduced *in situ* upon the addition of 1 equiv of *n*-OctMgCl to generate the same Ni^{I} species **4** (Figure S40), although to a lower extent for **1**, which may explain why **1** generates lower yields of the coupled product (Table 2, entry 9). One of the possible mechanisms for Ni^{II} reduction by the Grignard reagent could be double transmetalation and reductive elimination to generate the homocoupled product (hexadecane), followed by comproportionation of the generated Ni^{0} with Ni^{II} to generate the Ni^{I} catalyst (Figure S51). Since Ni^{I} species does not undergo transmetalation, we hypothesized that the amount of hexadecane will only depend on the catalyst loading. Indeed, more hexadecane is formed as the catalyst loading is increased (Figure S52), where the yield of hexadecane formed is about half of the catalyst loading used in the reaction (especially if the equivalents of Grignard are increased proportionally to the catalyst loading), providing strong support for this proposed mechanism of Ni^{I} species generation.

We then probed the transmetalation and oxidative addition reactivity of **4** with either a Grignard reagent or an alkyl halide, respectively. Although the addition of *n*-OctMgCl to **4** led to no spectral changes (Figure 6B), the reaction of **4** with CH_3I generated a new EPR spectrum that is different from those of the independently

prepared complexes **3** and **4**. We propose that the new Ni^{III} species is a 6-coordinate $[(iPr_3TACN)Ni^{III}(Me)(I)(MeCN)]^+$ complex generated by the oxidative addition of CH_3I to **4**. The EPR spectrum was simulated using *g* values of 2.398, 2.274, and 2.001 along with superhyperfine coupling in the g_z direction corresponding to two N atoms (Figures 6C and S41). This oxidative addition step is similar to what was observed previously by Lipschutz et al.[60] and Manesis et al.[37] Subsequently, 1 equiv CH_3MgI was added to the resulting solution, leading to the generation of an EPR spectrum that is identical to the spectrum of the $Ni^{III}Me_2$ species **3** (Figures 6D and S42). Overall, these results strongly suggest that in this system, the Ni^{I} species undergoes oxidative addition with the alkyl halide first,[61] followed by transmetalation with the Grignard reagent at Ni^{III}. Combined with the direct observation of reductive elimination from a Ni^{III}-dialkyl species to generate a detectable Ni^{I} species and the C-C coupled product (Figures 2 and S35), this is, to the best of our knowledge, the first study in which all reactive intermediates involved in a Kumada cross-coupling mediated by a Ni^{I}/Ni^{III} catalytic cycle have been observed spectroscopically.

To probe whether alkyl radical species are formed during catalysis, the radical clock iodomethylcyclopropane was employed as the electrophile substrate, along with *n*-octylMgCl. This catalytic reaction led to the formation of the ring-opened cross-coupled product 1-dodecene in 86% yield and without the formation of any cyclic product (Figure 6E), supporting a radical mechanism. Moreover, performing the catalytic reaction in the presence of radical trap 2,2,6,6-tetramethylpiperidine-1-oxyl (TEMPO) led to almost complete ablation of productive cross-coupling, along with the formation of alkyl-TEMPO adducts (Table S6). The reaction of Ni^{I} species **4** with *n*-heptyl-I in the presence of TEMPO generated the *n*-heptyl-TEMPO adduct, suggesting the formation of alkyl radicals during the oxidative addition process. Overall, these results further support the formation of alkyl radicals during the Ni-catalyzed Csp^3-Csp^3 Kumada cross-coupling reaction.

Based on the mechanistic studies described above, the mechanism for the catalytic Kumada cross-coupling reaction is proposed to begin with the generation of the catalytically active Ni^{I}(MeCN) species (**A**) via the reduction of the Ni^{II} precursor by the Grignard reagent (Figure 6F). Oxidative addition of the alkyl halide to the Ni^{I} center can occur to generate a Ni^{III}(alkyl)halide(MeCN) species (**B**), either via a single electron transfer (SET) process or a concerted oxidative addition—although the generated Ni^{III} species **B** can undergo reversible homolytic cleavage of the Ni–alkyl bond. This generated Ni^{III} intermediate can then undergo transmetalation with the Grignard reagent to form the Ni^{III}-dialkyl species (**C**), followed by rapid reductive elimination of the C-C coupled product and regeneration of the Ni^{I} species to close the catalytic cycle.

Conclusions

In summary, herein, we report the synthesis, characterization, and reactivity studies of organometallic Ni complexes supported by the bulky tridentate ligand iPr_3TACN. These complexes are involved in well-defined oxidative addition, transmetalation, and reductive elimination steps that are essential to the cross-coupling catalytic cycle. Mechanistic studies involving EPR spectroscopy, electrochemical methods, and radical trap studies provide unambiguous evidence for a direct Csp^3-Csp^3 reductive elimination from Ni^{III} to Ni^{I}, oxidative addition of an alkyl halide via a radical mechanism from Ni^{I} and Ni^{III}, transmetalation at Ni^{III}, and the reduction of a Ni^{II} precatalyst to an active Ni^{I} species by the Grignard reagent. Moreover, $(iPr_3TACN)Ni^{II}$ complexes were shown to be efficient catalysts for the Csp^3-Csp^3 Kumada cross-coupling reaction. A surprising beneficial effect of

acetonitrile on the yield of the cross-coupled product was observed during the Ni-mediated coupling, either when iPr_3TACN or a range of other tridentate ligands were employed. Although the beneficial role of nitriles (mostly aryl nitriles) in Ni catalysis has been reported previously, such a role was proposed to be due to the formation of Ni^0-nitrile interactions.[31–36] Herein, detailed spectroscopic, electrochemical, and mechanistic studies suggest that weaker π-acceptors, such as acetonitrile and other alkyl nitriles, are able to slightly stabilize a Ni^I species while also preventing β-hydride elimination and promoting transmetalation and rapid reductive elimination from the Ni^{III} species. By contrast, in this system, the use of aryl nitriles or other π-acids has a significant detrimental effect on the cross-coupled product yield. Overall, these studies suggest that the presence of a coordinating solvent and a weak π-acceptor, such as acetonitrile, could have a beneficial effect for a range of Ni-mediated organometallic transformations involving Ni^I intermediates.

EXPERIMENTAL PROCEDURES

Resource availability

Lead contact

Information regarding experimental procedures and requests for resources, data, and reagents should be directed to the lead contact, Liviu M. Mirica (mirica@illinois.edu).

Materials availability

Full experimental details, including complex synthesis, spectroscopic characterization, NMR, high-resolution MS (HR-MS), EPR, and X-ray diffraction data, are available in the supplemental information for all unique compounds. All reagents in this study are either commercially available or can be prepared as indicated in the supplemental information.

Data and code availability

Crystallographic data for complexes **1**, **2**, and **4** have been deposited at the Cambridge Crystallographic Data Centre (CCDC). The CCDC deposition numbers are 2182915 (**1**), 2182916 (**2**), and 2182917 (**4**). All data supporting this study are available in the manuscript and supplemental information. Additional information is available from the lead contact upon request.

SUPPLEMENTAL INFORMATION

Supplemental information can be found online at https://doi.org/10.1016/j.chempr.2023.11.008.

ACKNOWLEDGMENTS

We thank the National Science Foundation (CHE-1925751 and CHE-2155160 to L.M.M.) for support. We also thank Prof. Nigam Rath from the University of Missouri, St. Louis, USA for assisting with solving the crystal structures of complexes **1** and **2**. We thank Dr. Hanah Na for assistance with calculating the spin density of Ni complexes and Bailey S. Bouley for generating the original TOC graphic.

AUTHOR CONTRIBUTIONS

L.G. synthesized the ligand and metal complexes and performed spectroscopic studies. J.B.C. performed the catalytic reactions and mechanistic studies. L.M.M. performed the DFT calculations. L.G. and J.B.C. collected and interpreted all data. L.G., J.B.C., and L.M.M. wrote the manuscript.

DECLARATION OF INTERESTS

The authors declare no competing interests.

INCLUSION AND DIVERSITY

We support inclusive, diverse, and equitable conduct of research. One or more of the authors of this paper self-identifies as an underrepresented ethnic minority in their field of research or within their geographical location.

Received: May 31, 2023
Revised: July 19, 2023
Accepted: November 20, 2023
Published: December 14, 2024

REFERENCES

1. Campeau, L.C., and Hazari, N. (2019). Cross-coupling and related reactions: connecting past success to the development of new reactions for the future. Organometallics *38*, 3–35.

2. Diccianni, J.B., and Diao, T. (2019). Mechanisms of nickel-catalyzed cross-coupling reactions. J. Trends Chem. *1*, 830–844.

3. Choi, J., and Fu, G.C. (2017). Transition metal-catalyzed alkyl-alkyl bond formation: another dimension in cross-coupling chemistry. Science *356*, eaaf7230.

4. Tasker, S.Z., Standley, E.A., and Jamison, T.F. (2014). Recent advances in homogeneous nickel catalysis. Nature *509*, 299–309.

5. Hu, X. (2011). Nickel-catalyzed cross coupling of non-activated alkyl halides: a mechanistic perspective. Chem. Sci. *2*, 1867–1886.

6. Zhou, J.S., and Fu, G.C. (2003). Cross-couplings of unactivated secondary alkyl halides: room-temperature nickel-catalyzed Negishi reactions of alkyl bromides and iodides. J. Am. Chem. Soc. *125*, 14726–14727.

7. Anderson, T.J., Jones, G.D., and Vicic, D.A. (2004). Evidence for a Ni-I active species in the catalytic cross-coupling of alkyl electrophiles. J. Am. Chem. Soc. *126*, 8100–8101.

8. Jones, G.D., McFarland, C., Anderson, T.J., and Vicic, D.A. (2005). Analysis of key steps in the catalytic cross-coupling of alkyl electrophiles under Negishi-like conditions. Chem. Commun. (Camb), 4211–4213.

9. Jones, G.D., Martin, J.L., McFarland, C., Allen, O.R., Hall, R.E., Haley, A.D., Brandon, R.J., Konovalova, T., Desrochers, P.J., Pulay, P., et al. (2006). Ligand redox effects in the synthesis, electronic structure, and reactivity of an alkyl-alkyl cross-coupling catalyst. J. Am. Chem. Soc. *128*, 13175–13183.

10. Vechorkin, O., and Hu, X. (2009). Nickel-catalyzed cross-coupling of non-activated and functionalized alkyl halides with alkyl Grignard reagents. Angew. Chem. Int. Ed. Engl. *48*, 2937–2940.

11. Shi, R., Zhang, Z., and Hu, X. (2019). Nickamine and analogous nickel pincer catalysts for cross-coupling of alkyl halides and hydrosilylation of alkenes. Acc. Chem. Res. *52*, 1471–1483.

12. Yin, H., and Fu, G.C. (2019). Mechanistic investigation of enantioconvergent Kumada reactions of racemic alpha-bromoketones catalyzed by a nickel/bis(oxazoline) complex. J. Am. Chem. Soc. *141*, 15433–15440.

13. Bour, J.R., Camasso, N.M., Meucci, E.A., Kampf, J.W., Canty, A.J., and Sanford, M.S. (2016). Carbon–carbon bond-forming reductive elimination from isolated nickel(III) complexes. J. Am. Chem. Soc. *138*, 16105–16111.

14. Roberts, C.C., Camasso, N.M., Bowes, E.G., and Sanford, M.S. (2019). Impact of oxidation state on reactivity and selectivity differences between nickel(III) and nickel(IV) alkyl complexes. Angew. Chem. Int. Ed. Engl. *58*, 9104–9108.

15. Bour, J.R., Ferguson, D.M., McClain, E.J., Kampf, J.W., and Sanford, M.S. (2019). Connecting organometallic Ni(III) and Ni(IV): reactions of carbon-centered radicals with high-valent organonickel complexes. J. Am. Chem. Soc. *141*, 8914–8920.

16. Zheng, B., Tang, F.Z., Luo, J., Schultz, J.W., Rath, N.P., and Mirica, L.M. (2014). Organometallic nickel(III) complexes relevant to cross-coupling and carbon-heteroatom bond formation reactions. J. Am. Chem. Soc. *136*, 6499–6504.

17. Tang, F.Z., Rath, N.P., and Mirica, L.M. (2015). Stable bis(trifluoromethyl)nickel(III) complexes. Chem. Commun. (Camb) *51*, 3113–3116.

18. Schultz, J.W., Fuchigami, K., Zheng, B., Rath, N.P., and Mirica, L.M. (2016). Isolated organometallic nickel(III) and nickel(IV) complexes relevant to carbon-carbon bond formation reactions. J. Am. Chem. Soc. *138*, 12928–12934.

19. Watson, M.B., Rath, N.P., and Mirica, L.M. (2017). Oxidative C–C bond formation reactivity of organometallic Ni(II), Ni(III), and Ni(IV) complexes. J. Am. Chem. Soc. *139*, 35–38.

20. Smith, S.M., Rath, N.P., and Mirica, L.M. (2019). Axial donor effects on oxidatively induced ethane formation from nickel–dimethyl complexes. Organometallics *38*, 3602–3609.

21. Sessler, J.L., Sibert, J.W., and Lynch, V. (1994). Bulky substituent effects on the iron(III) complexation of 1,4,7-triazacyclononane. Inorg. Chim. Acta *216*, 89–95.

22. Lam, B.M.T., Halfen, J.A., Young, V.G., Hagadorn, J.R., Holland, P.L., Lledós, A., Cucurull-Sánchez, L., Novoa, J.J., Alvarez, S., and Tolman, W.B. (2000). Ligand macrocycle structural effects on copper-dioxygen reactivity. Inorg. Chem. *39*, 4059–4072.

23. Han, W., Li, L., Liu, Z.Q., Yan, S.P., Liao, D.Z., Jiang, Z.H., and Shen, P.W. (2004). Synthesis, structure, and spectroscopic properties of copper(II) and nickel(II) complexes containing the 1, 4, 7-triisopropyl-1, 4, 7-triazacyclononane ligand. Z. Anorg. Allg. Chem. *630*, 591–596.

24. Bossek, U., Nühlen, D., Bill, E., Glaser, T., Krebs, C., Weyhermüller, T., Wieghardt, K., Lengen, M., and Trautwein, A.X. (1997). Exchange coupling in an isostructural series of face-sharing bioctahedral complexes $[LM^{II}(\mu\text{-}X)_3M^{II}L]BPh_4$ (M = Mn, Fe, Co, Ni, Zn; X=Cl, Br; L = 1,4,7-trimethyl-1,4,7-triazacyclononane). Inorg. Chem. *36*, 2834–2843.

25. Rebilly, J.N., Charron, G., Riviere, E., Guillot, R., Barra, A.L., Serrano, M.D., van Slageren, J., and Mallah, T. (2008). Large magnetic anisotropy in pentacoordinate Ni-II complexes. Chem. Eur. J. *14*, 1169–1177.

26. Thangavel, A., Wieliczko, M., Bacsa, J., and Scarborough, C.C. (2013). 1,4,7-triazacyclononane ligands bearing tertiary alkyl nitrogen substituents. Inorg. Chem. *52*, 13282–13287.

27. Khusnutdinova, J.R., Rath, N.P., and Mirica, L.M. (2012). The aerobic oxidation of a Pd(II) dimethyl complex leads to selective ethane elimination from a Pd(III) intermediate. J. Am. Chem. Soc. *134*, 2414–2422.

28. Khusnutdinova, J.R., Qu, F., Zhang, Y., Rath, N.P., and Mirica, L.M. (2012). Formation of the Pd(IV) complex $[(Me_3tacn)Pd^{IV}Me_3]^+$ through aerobic oxidation of $(Me_3tacn)Pd^{II}Me_2$ (Me_3tacn = N,N′,N″-trimethyl-1,4,7-triazacyclononane). Organometallics *31*, 4627–4630.

29. Haselhorst, G., Stoetzel, S., Strassburger, A., Walz, W., Wieghardt, K., and Nuber, B. (1993). Synthesis and co-ordination chemistry of the macrocycle 1,4,7-triisopropyl-1,4,7-triazacyclononane. J. Chem. Soc. Dalton Trans. *1*, 83–90.

30. Griego, L., Woods, T.J., and Mirica, L.M. (2022). A five-coordinate Ni(I) complex supported by 1,4,7-triisopropyl-1,4,7-triazacyclononane. Chem. Commun. (Camb) *58*, 7360–7363.

31. Ge, S.Z., and Hartwig, J.F. (2011). Nickel-catalyzed asymmetric alpha-arylation and heteroarylation of ketones with chloroarenes: effect of halide on selectivity, oxidation state, and room-temperature reactions. J. Am. Chem. Soc. *133*, 16330–16333.

32. Ge, S., Green, R.A., and Hartwig, J.F. (2014). Controlling first-row catalysts: amination of aryl and heteroaryl chlorides and bromides with primary aliphatic amines catalyzed by a BINAP-ligated single-component Ni(0) complex. J. Am. Chem. Soc. *136*, 1617–1627.

33. Green, R.A., and Hartwig, J.F. (2015). Nickel-catalyzed amination of aryl chlorides with ammonia or ammonium salts. Angew. Chem. Int. Ed. Engl. *54*, 3768–3772.

34. Yin, G.Y., Kalvet, I., Englert, U., and Schoenebeck, F. (2015). Fundamental studies and development of nickel-catalyzed trifluoromethylthiolation of aryl chlorides: active catalytic species and key roles of ligand and traceless MeCN additive revealed. J. Am. Chem. Soc. *137*, 4164–4172.

35. Mills, L.R., Edjoc, R.K., and Rousseaux, S.A.L. (2021). Design of an electron-withdrawing benzonitrile ligand for Ni-catalyzed cross-coupling involving tertiary nucleophiles. J. Am. Chem. Soc. *143*, 10422–10428.

36. Saputra, L., Arifin, Gustini, N., Sinambela, N., Indriyani, N.P., Sakti, A.W., Arrozi, U.S.F., Martoprawiro, M.A., Patah, A., and Permana, Y. (2022). Nitrile modulated-Ni(0) phosphines in trans-selective phenylpropenoids isomerization: an allylic route by a regular η1-N(end-on) or an alkyl route via a flipped-nitrile? Mol. Catal. *533*, 112768.

37. Manesis, A.C., Musselman, B.W., Keegan, B.C., Shearer, J., Lehnert, N., and Shafaat, H.S. (2019). A biochemical nickel(I) state supports nucleophilic alkyl addition: a roadmap for methyl reactivity in acetyl coenzyme A synthase. Inorg. Chem. *58*, 8969–8982.

38. Ragsdale, S.W., Ljungdahl, L.G., and Dervartanian, D.V. (1983). ^{13}C and ^{61}Ni isotope substitutions confirm the presence of a nickel(III)-carbon species in acetogenic Co dehydrogenases. Biochem. Biophys. Res. Commun. *115*, 658–665.

39. Lin, C.Y., and Power, P.P. (2017). Complexes of Ni(I): a "rare" oxidation state of growing importance. Chem. Soc. Rev. *46*, 5347–5399.

40. Bassi, I.W., Benedicenti, C., Calcaterra, M., and Rucci, G. (1976). Preparation and x-ray crystal structure of (benzonitrile) tris(triphenylphosphorane)nickel(0). J. Organomet. Chem. *117*, 285–295.

41. Bassi, I.W., Benedicenti, C., Calcaterra, M., Intrito, R., Rucci, G., and Santini, C. (1978). X-ray crystal structure of the clathrate compound tetrakis[(benzonitrile)(triphenylphosphorane) nickel(0)] · 2 toluene · ∼1 n-hexane · ∼1 cycloocta-1,5-diene. J. Organomet. Chem. *144*, 225–237.

42. Garcia, J.J., and Jones, W.D. (2000). Reversible cleavage of carbon-carbon bonds in benzonitrile using nickel(0). Organometallics *19*, 5544–5545.

43. Garcia, J.J., Brunkan, N.M., and Jones, W.D. (2002). Cleavage of carbon-carbon bonds in aromatic nitriles using nickel(0). J. Am. Chem. Soc. *124*, 9547–9555.

44. Stolley, R.M., Duong, H.A., Thomas, D.R., and Louie, J. (2012). The discovery of [Ni(NHC)RCN]$_2$ species and their role as cycloaddition catalysts for the formation of pyridines. J. Am. Chem. Soc. *134*, 15154–15162.

45. Walther, D., Schönberg, H., Dinjus, E., and Sieler, J. (1987). Aktivierung von Kohlendioxid an Übergangsmetallzentren: selektive Cooligomerisation mit Hexin(−3) durch das Katalysatorsystem Acetonitril/Trialkylphosphan/Nickel(0) und Struktur eines nickel(0)-Komplexes mit side-on gebundenem Acetonitril. J. Organomet. Chem. *334*, 377–388.

46. Ateşin, T.A., Li, T., Lachaize, S., Brennessel, W.W., García, J.J., and Jones, W.D. (2007). Experimental and theoretical examination of C−CN and C−H bond activations of acetonitrile using zerovalent nickel. J. Am. Chem. Soc. *129*, 7562–7569.

47. Afandiyeva, M., Kadam, A.A., Wu, X., Brennessel, W.W., and Kennedy, C.R. (2022). Synthesis, structure, and hydroboration reactivity of anionic nickel(0) complexes supported by bidentate NHC-pyridone ligands. Organometallics *41*, 3014–3023.

48. Johnson, K.A., Biswas, S., and Weix, D.J. (2016). Cross-electrophile coupling of vinyl halides with alkyl halides. Chemistry *22*, 7399–7402.

49. Biswas, S., Qu, B., Desrosiers, J.N., Choi, Y., Haddad, N., Yee, N.K., Song, J.J., and Senanayake, C.H. (2020). Nickel-catalyzed cross-electrophile reductive couplings of neopentyl bromides with aryl bromides. J. Org. Chem. *85*, 8214–8220.

50. Pang, X., Zhao, Z.Z., Wei, X.X., Qi, L., Xu, G.L., Duan, J., Liu, X.Y., and Shu, X.Z. (2021). Regiocontrolled reductive vinylation of aliphatic 1,3-dienes with vinyl triflates by nickel catalysis. J. Am. Chem. Soc. *143*, 4536–4542.

51. Claros, M., Ungeheuer, F., Franco, F., Martin-Diaconescu, V., Casitas, A., and Lloret-Fillol, J. (2019). Reductive cyclization of unactivated alkyl chlorides with tethered alkenes under visible-light photoredox catalysis. Angew. Chem. Int. Ed. Engl. *58*, 4869–4874.

52. Aragón, J., Sun, S., Pascual, D., Jaworski, S., and Lloret-Fillol, J. (2022). Photoredox activation of inert alkyl chlorides for the reductive cross-coupling with aromatic alkenes. Angew. Chem. Int. Ed. Engl. *61*, e202114365.

53. Dawson, D.D., Oswald, V.F., Borovik, A.S., and Jarvo, E.R. (2020). Identification of the active catalyst for nickel-catalyzed stereospecific Kumada coupling reactions of ethers. Chemistry *26*, 3044–3048.

54. Pearson-Long, M.S.M., Boeda, F., and Bertus, P. (2017). Double addition of organometallics to nitriles: toward an access to tertiary carbinamines. Adv. Synth. Catal. *359*, 179–201.

55. Zhou, W., Schultz, J.W., Rath, N.P., and Mirica, L.M. (2015). Aromatic methoxylation and hydroxylation by organometallic high-valent nickel complexes. J. Am. Chem. Soc. *137*, 7604–7607.

56. Smith, S.M., Planas, O., Gómez, L., Rath, N.P., Ribas, X., and Mirica, L.M. (2019). Aerobic C-C and C-O bond formation reactions mediated by high-valent nickel species. Chem. Sci. *10*, 10366–10372.

57. Na, H., Watson, M.B., Tang, F., Rath, N.P., and Mirica, L.M. (2021). Photoreductive chlorine elimination from a Ni(III)Cl$_2$ complex supported by a tetradentate pyridinophane ligand. Chem. Commun. (Camb) *57*, 7264–7267.

58. Na, H., and Mirica, L.M. (2022). Deciphering the mechanism of the Ni-photocatalyzed C−O cross-coupling reaction using a tridentate pyridinophane ligand. Nat. Commun. *13*, 1313.

59. Reisenbauer, J.C., Finkelstein, P., Ebert, M.O., and Morandi, B. (2023). Mechanistic investigation of the nickel-catalyzed transfer hydrocyanation of alkynes. ACS Catal. *13*, 11548–11555.

60. Lipschutz, M.I., Yang, X., Chatterjee, R., and Tilley, T.D. (2013). A structurally rigid bis(amido) ligand framework in low-coordinate Ni(I), Ni(II), and Ni(III) analogues provides access to a Ni(III) methyl complex via oxidative addition. J. Am. Chem. Soc. *135*, 15298–15301.

61. Ting, S.I., Williams, W.L., and Doyle, A.G. (2022). Oxidative addition of aryl halides to a Ni(I)-bipyridine complex. J. Am. Chem. Soc. *144*, 5575–5582.